Available online at www.sciencedirect.com

ScienceDirect

Applied Mathematical Modelling 32 (2008) 535–546

APPLIED MATHEMATICAL MODELLING

www.elsevier.com/locate/apm

Numerical solutions of KdV equation using radial basis functions

İdris Dağ [a,*], Yılmaz Dereli [b]

[a] Mathematics Department, Eskişehir Osmangazi University, 26480 Eskişehir, Turkey
[b] Mathematics Department, Anadolu University, 26470 Eskişehir, Turkey

Received 21 September 2006; received in revised form 31 January 2007; accepted 6 February 2007
Available online 14 February 2007

Abstract

Numerical solution of the Korteweg-de Vries equation is obtained by using the meshless method based on the collocation with radial basis functions. Five standard radial basis functions are used in the method of the collocation. The results are compared for the numerical experiments of the propagation of solitons, interaction of two solitary waves and breakdown of initial conditions into a train of solitons.

Keywords: Radial basis functions; KdV equation

1. Introduction

Korteweg-de Vries equation (KDVE) is a nonlinear partial differential equation, which is initially introduced to describe the lossless propagation of shallow water waves [1]. It represents the long time evolution of wave phenomena, in which the effect of the nonlinear terms UU_x is counterbalanced by the dispersion U_{xxx}. Thus it has been found to model many wave phenomena such as waves in enharmonic crystals, bubble liquid mixtures, ion acoustic wave and magnetohydrodynamic waves in a warm plasma as well as shallow water waves [1–5]. The KDVE exhibits solutions such as solitary waves, solitons and recurrence [2]. The KDVE is a completely integrable Hamiltonian system which can solved explicitly. Thus some analytical solutions of the KDVE are found, and their existence and uniqueness have been studied for a certain class of initial functions [2]. Usefulness of these solutions in general is limited. Therefore the numerical solutions of the KDVE are essential because of solution which are not analytically available. Many methods have been proposed for numerical treatment of the KDVE for the various boundary and initial conditions. The numerical method proposed by calculating the solution of the KDVE must possess at least two properties. Ideally a numerical method should be free of phase errors and the conservation properties of the equation must be

* Corresponding author. Tel.: +90 2222269462.
E-mail address: idag@ogu.edu.tr (İ. Dağ).

0307-904X/$ - see front matter
doi:10.1016/j.apm.2007.02.001

satisfied. Since the KDVE is an integrable Hamiltonian system, then there exists infinitely many independent conserved quantities. We will observe the well-known four conserved quantities of the KDVE for our numerical solutions.

The numerical solutions of the partial differential equations can be found by using the techniques known as the finite element, finite difference and spectral methods. However difficulty of mesh generation, especially two or tree dimensional problems, makes these methods a difficult task to apply for finding the numerical solution of the differential equations. In addition, these methods require regular grid system, which makes it very difficult to model the detailed topographic features of an irregular domain and are not well suited to the problems associated with extremely large deformation. In the last decade, meshless method has gained quite importance to get the numerical solution of the various types of partial differential equations. So the development of the meshless method is required to alleviate the meshing problems associated with methods such as the finite element and finite difference. Various meshless methods have been developed. Meshless method based on the collocation method has been dominant and very efficient. They have been successfully applied as tool for collocation of the differential equations since initial development of Kansa' work [6]. Some papers have been written to solve partial differential equations using the collocation method with different radial basis functions [7–12]. The choice of radial basis functions (RBF) is a flexible feature of meshless methods. The RBF can be globally supported, infinitely differentiable, and contain free parameters, called shape parameters, which affect both accuracy of the solutions and conditioning of the collocation matrix. Optimal shape parameters, which mean the value of the shape parameter that can produces the most accurate results have been found by searching a value from selected random regions. But the optimal choice of the shape parameters is still an open problem. In our calculation, we have selected the optimal shape parameters by brute-force as well. Some type of the RBF have been intensively used in forming the collocation method for a solution of partial differential equations. The mathematical theory of the RBF has lagged back behind the numerical applications to PDE. But recently there has been some progress on dealing with convergence of some types of the RBF methods in the papers [13–16]. Error estimates for the collocation method with the RBF have been given for the linear PDE [8,17]. There has been not much work done on the convergency of the collocation method with the RBF functions in solving the time-dependent PDE. In this paper, we have expanded the use of the RBF on the numerical solutions of the KDVE with propagation of soliton, solitons interaction and evolution of solitons. Thus the collocation method with some five standard radial basis functions is applied in finding the numerical solution of the KDVE. The effect of the radial basis functions in the collocation method is investigated. In Section 2, The collocation algorithm is introduced for the solution of the KDVE. Then several numerical experiments are presented in section of the numerical results.

2. The governing equation and radial basis method

We consider the Korteweg-de Vries equation

$$U_t + \varepsilon U U_x + \mu U_{xxx} = 0 \tag{1}$$

with boundary conditions $\frac{\partial U}{\partial x} \to 0$ as $|\, x \,| \to 0$ and initial conditions

$$U(x,0) = f(x), \tag{2}$$

where ε, μ are positive parameters and subscripts x and t denote differentiation. We look for the solution on $[a,b] \times [0,T]$ for computational purposes. When the solution remain negligibly small at both boundaries a and b, the spatial interval $[a,b]$ can be chosen sufficiently large to carry on the numerical experiment during the time of interval $[0,T]$

$$U(a,t) = \alpha_1, \quad U(b,t) = \alpha_2, \qquad a \leqslant x \leqslant b, \;\; t \geqslant 0. \tag{3}$$

We discretize time derivative of the KDVE by using usual finite difference formula and space derivative by the Crank–Nicolson formula between successive two time levels n and $n+1$

$$\frac{U^{n+1} - U^n}{\Delta t} + \varepsilon \frac{(UU_x)^{n+1} + (UU_x)^n}{2} + \mu \frac{(U_{xxx})^{n+1} + (U_{xxx})^n}{2} = 0. \tag{4}$$

The nonlinear term in the above equation is linearized by using the following term [18]:

$$(UU_x)^{n+1} = U^{n+1}(U_x)^n + U^n(U_x)^{n+1} - U^n(U_x)^n \tag{5}$$

So time-discretized KDVE (4) can be written as

$$U^{n+1} + \varepsilon\frac{\Delta t}{2}\left(U^n(U_x)^{n+1} + (U_x)^n U^{n+1}\right) + \mu\frac{\Delta t}{2}(U_{xxx})^{n+1} = U^n - \mu\frac{\Delta t}{2}(U_{xxx})^n. \tag{6}$$

To apply the collocation method using radial basis functions, let us choose the collocation point $x_i,\ i = 0,\dots,N$ over the problem domain $[a,b]$ of which $x_i,\ i = 1,\dots,N-1$ are interior points, $x_i,\ i = 0,N$ are boundary points. An approximate solution to the analytic solution U in Eq. (1) is sought in a form

$$U_N(x) = \sum_{j=0}^{N}\lambda_j\phi(r_j), \tag{7}$$

where λ's are the coefficients to be determined, N is the number of data points. ϕ is some form of the radial basis functions. $r_j = |x - x_j|$ denotes the Euclidean norm between collocation points x and x_j. x_j are known as the centers being given *distinct* point in the interval $[a,b]$. Most-widely used radial basis functions are the following:

Multiquadric(MQ)	$\phi(r_j) = \sqrt{r_j^2 + c^2}$,
Inverse multiquadric(IMQ)	$\phi(r_j) = 1\Big/\sqrt{r_j^2 + c^2}$,
Inverse quadric(IQ)	$\phi(r_j) = 1\Big/(r_j^2 + c^2)$,
Thin plate spline(TPS)	$\phi(r_j) = r_j^2\log(r_j)$,
Gaussian(G)	$\phi(r_j) = e^{-c^2 r_j^2}$,

where c is the shape parameter of the radial basis functions. Optimal shape values are found experimentally and these values are written for each text problems. By substituting Eq. (7) into Eqs. (2) and (6) and the collocation points $x_i,\ i = 0,\dots,N$ in place of x, we obtain following equations:

$$\begin{aligned}\sum_{j=0}^{N}\lambda_j^{n+1}\phi(r_{ij}) &+ \varepsilon\frac{\Delta t}{2}\left(\sum_{j=0}^{N}\lambda_j^n\phi'(r_{ij})\sum_{j=0}^{N}\lambda_j^{n+1}\phi(r_{ij}) + \sum_{j=0}^{N}\lambda_j^n\phi(r_{ij})\sum_{j=0}^{N}\lambda_j^{n+1}\phi'(r_{ij})\right)\\ &+ \mu\frac{\Delta t}{2}\sum_{j=0}^{N}\lambda_j^{n+1}\phi'''(r_{ij}) = \sum_{j=0}^{N}\lambda_j^n\phi(r_{ij}) - \mu\frac{\Delta t}{2}\sum_{j=0}^{N}\lambda_j^n\phi'''(r_{ij})\end{aligned} \tag{8}$$

and

$$\sum_{j=0}^{N}\lambda_j^{n+1}\phi(r_{ij}) = \alpha_i, \quad i = 0,N. \tag{9}$$

Eqs. (8) and (9) generates a system of $(N+1)$ linear equations in $(N+1)$ unknown parameters λ_j^{n+1}. In the above system, the centers and collocation points have been chosen as the same except for the use of thin plate spline radial basis functions on the meshless method. The collocation matrix becomes ill-conditioned during the run of the algorithms for the thin plate spline radial basis functions. Slightly different choices of these points gives a solvable system. Before solving the system, boundary conditions $U(a,t) = \alpha_1,\ U(b,t) = \alpha_2$ are applied to the system so that a system of $N \times N$ equations is obtained. The system is solved with the Gaussian elimination method with partial pivoting. The approximate solution can be obtained from Eq. (7) at any point in the problem domain after finding the unknown coefficients $\lambda_j^n,\ j = 1,\dots N$ at each time steps.

3. Numerical examples and comparisons

Miura et al. [19] have shown that there are an infinite number of conservation laws for the KDVE. We have calculated the first four conservations

$$I_1 = \int_{-\infty}^{\infty} U\,\mathrm{d}x, \quad I_2 = \int_{-\infty}^{\infty} U^2\,\mathrm{d}x, \quad I_3 = \int_{-\infty}^{\infty} \left(U^3 - \frac{3}{\varepsilon}\mu(U_x)^2\right)\mathrm{d}x,$$
$$I_4 = \int_{-\infty}^{\infty} \left(U^4 - \frac{12}{\varepsilon}\mu U(U_x)^2 + \frac{36}{5\varepsilon^2}\mu^2(U_{xx})^2\right)\mathrm{d}x \tag{10}$$

The method has been validated by studying test problems concerning with the migration, interaction and generation of solitons. We use the L_2 and L_∞ error norms to measure the difference between the numerical and analytical solutions and hence to show how well the scheme predicts the position and amplitude of solution as the simulation proceeds. The L_2 error norm defined as

$$L_2 = \|U^{\text{exact}} - U_N\|_2 = \sqrt{h\sum_{j=0}^{N}|U_j^{\text{exact}} - (U_N)_j|^2} \tag{11}$$

and L_∞ error norm defined as

$$L_\infty = \|U^{\text{exact}} - U_N\|_\infty = \max_j |U_j^{\text{exact}} - (U_N)_j| \tag{12}$$

will be calculated to examine accuracy of proposed algorithms.

3.1. Test problem 1

We wish to solve the KDVE with the following initial condition:

$$U(x,0) = 3c\sec h^2(Ax + D)$$

and boundary conditions

$$U(0,t) = U(2,t) = 0, \quad t > 0.$$

The analytical solution of the KDVE is

$$U(x,t) = 3c\sec h^2(Ax - Bt + D), \tag{13}$$

where

$$A = \frac{1}{2}(\varepsilon c/\mu)^{1/2} \quad \text{and} \quad B = \frac{1}{2}\varepsilon cA.$$

The above solution represents a single soliton with amplitude $3c$, initially centered at $x = 0$, moving from left to the right with constant speed εc. To have admissible numerical solutions, the amplitude of the solitons must be represented faithfully for many time steps in calculations.

Computation was done with parameters $\varepsilon = 1,\ \mu = 4.84 \times 10^{-4},\ c = 0.3,\ D = -6$. Single soliton solution was carried out on the interval $[a,b] = [0,3]$ from $t = 0$ to $t = 3$ with space step $h = 0.01$ and time step $\Delta t = 0.005$. The L_2 and L_∞-error norms and conservation are illustrated in Table 1. The collocation method with MQ and G types of radial basis functions provides higher accuracy than that with IMQ, IQ and TPS. Analytical invariants conserve most with the collocation method with MQ. Amplitude of the soliton and location of peak of the soliton are also given in the same table at time $t = 3$. Peak position of the soliton for the method with radial basis functions remain the same as 1.38. The absolute difference between analytical and numerical soliton height is found as 0.000396 for MQ, 0.000221 for IMQ, 0.000447 for IQ, 0.001506 for TPS and 0.000514 for G. Numerical solutions with five radial basis functions at some times are graphed in Fig. 1. The solution curves are indistinguishable. Maximum error variations of the algorithm with different radial basis functions are depicted in Fig. 2 at time $t = 3$. Maximum errors occurs around the summit of

Table 1
Single soliton $h = 0.01,\ \Delta t = 0.005,\ t = 3$

Method	I_1	I_2	I_3	I_4	$L_2 \times 10^3$	$L_\infty \times 10^3$	Height	Position
MQ	0.144606	0.086759	0.046850	0.024094	0.062	0.133	0.899604	1.38
IMQ	0.144623	0.086765	0.046847	0.023869	2.751	5.018	0.902210	1.38
IQ	0.144598	0.086759	0.046849	0.023869	1.013	2.090	0.900447	1.38
TPS	0.144261	0.086762	0.046842	0.024012	2.606	6.345	0.898494	1.38
G	0.144601	0.086760	0.046850	0.023871	0.046	0.136	0.899486	1.38
Analytic ($t = 0$)	0.144598	0.086759	0.046850	0.024094			0.9	1.38

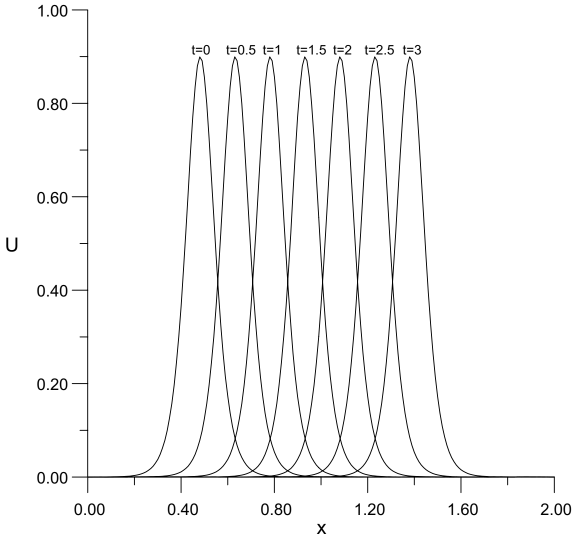

Fig. 1. A single solution. The progress of solitary wave from time 0 to 3.0.

the soliton. Overall, the computed results show that the method with the MQ radial basis function is the most efficient for single soliton experiment. The proposed method with G radial basis function is the second most efficient in finding the single soliton solution of the KDVE. The comparison of the results is done with some results of the methods listed in Table 2 when the space and time increments, $h = 0.01$, $\Delta t = 0.005$ are used. The proposed algorithm with both MQ and G radial basis functions gives the same results with method of Galerkin method based on quadratic B-spline functions [20] and better results than the finite differences [21] and Galerkin finite element methods [22,23]. The best results are obtained when the optimal shape values $c = 0.00041, 5000, 0.0025, 0.00335, 0.00025$ are used for MQ, G, IMQ, IQ and TPS radial basis functions, respectively.

3.2. Test problem 2

The second part of the numerical study deals with two soliton interaction solution of the KDVE. The linear sum of two separated solitons of various amplitudes is considered as the initial condition

$$U(x,t) = 3c_1 \sec h^2(A_1 x + D_1) + 3c_2 \sec h^2(A_2 x + D_2), \quad A_i = \frac{1}{2}(\varepsilon c_i/\mu_i)^{1/2}, \ \ i = 1,2$$

and the boundary conditions $U(a,t) = U(b,t) = 0$ are used. In this experiment, the behavior of the two solitons with different amplitudes travelling in the same direction is observed to pass through each other and then emerge unchanged. The solution represents two solitons of magnitudes c_1 and c_2 cited initially at $x = -D_1/A_1$

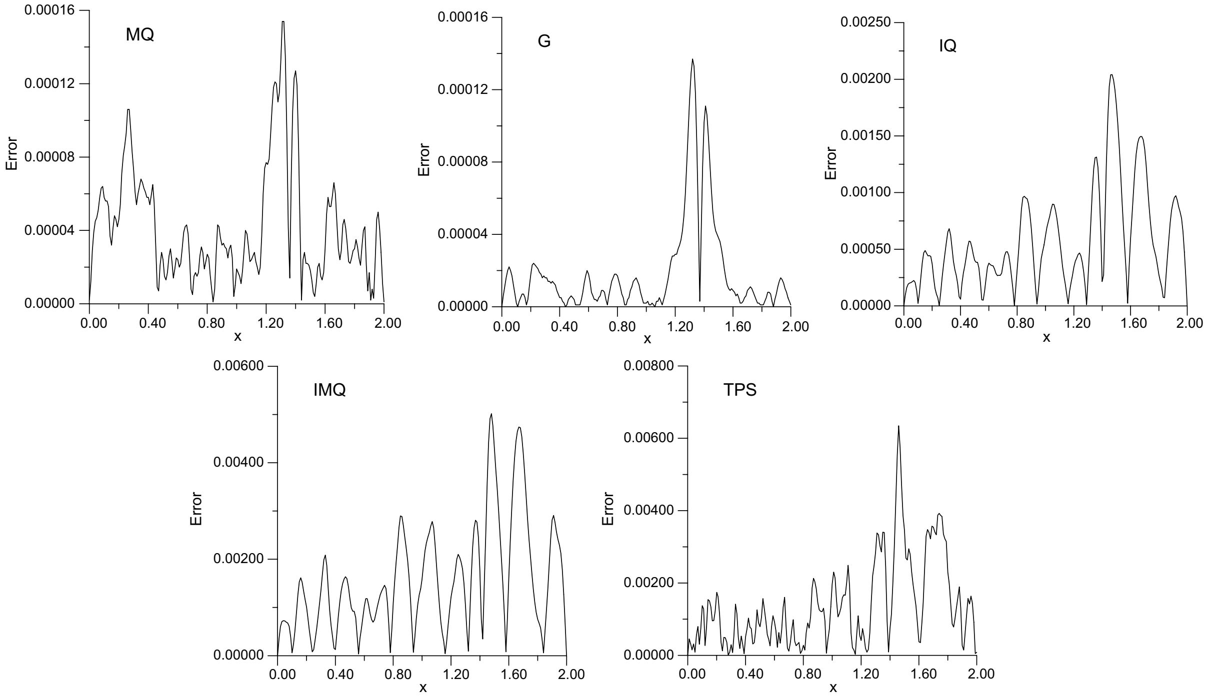

Fig. 2. Errors (numerical–analytical solution) at time $t = 3$.

Table 2
L_2-error$\times 10^3$, $h = 0.01$

Time	Zabusky–Kruskal [21]	Hopscoth [22] Galerkin quad spline [20]	Petrov Galerkin [23]	Modified P-G [23]	
	$\Delta t = 0.0005$		$\Delta t = 0.005$		
0.25	5.94	3.79	0.02	4.46	0.21
0.50	13.17	9.28	0.04	7.01	0.38
0.75	21.08	14.14	0.05	10.08	0.57
1.00	28.66	18.72	0.06	13.26	0.74
	MQ	G	IMQ	IQ	TPS
	$\Delta t = 0.005$				
0.25	0.0137	0.0218	1.3856	0.4880	3.1106
0.50	0.0192	0.0238	1.8558	0.6368	3.2264
0.75	0.0229	0.0263	2.0865	0.7125	3.8907
1.00	0.0260	0.0267	2.2104	0.7541	4.3381

and $-D_2/A_2$, respectively. Choosing $c_1 > c_2$ ensures that the velocity, and magnitude of soliton at $x = -D_1/A_1$ is the larger and ensures that the solitons interact with increasing time. Soliton interaction problem was solved on the interval $[0, 2]$ for $t = 0$ to $t = 3$ with $c_1 = 0.3,\ c_2 = 0.1,\ D_1 = 0,\ D_2 = 0$, time step $\Delta t = 0.005$ and space step $h = 0.002$. With this parameters, the soliton having larger amplitude $= 0.9$ are located to the left of the smaller one having the amplitude 0.3. Since the velocity of the solitons depends upon their magnitudes, the larger soliton passes through the smaller one as time advances. This has been shown in Fig. 3 at some times. Amplitudes of both solitons against time are illustrated in Fig. 4 for the algorithm. Invariant values I_1, I_2, I_3, I_4 during the simulation are given in Table 3 from which invariants for various basis functions remain satisfactorily conserved. Change in the invariants I_1, I_2, I_3, I_4 is smallest for the MQ and is less than 0.004%, 0.002%, 0.007%, 0.002%, respectively. Largest change is found by less than 0.01%, 0.002%, 0.003%, 0.02% for the invariants I_1, I_2, I_3, I_4, respectively, when TPS radial basis functions is employed in the collocation method. Best accuracy is found by use of optimal shape parameters $c = 0.1$,

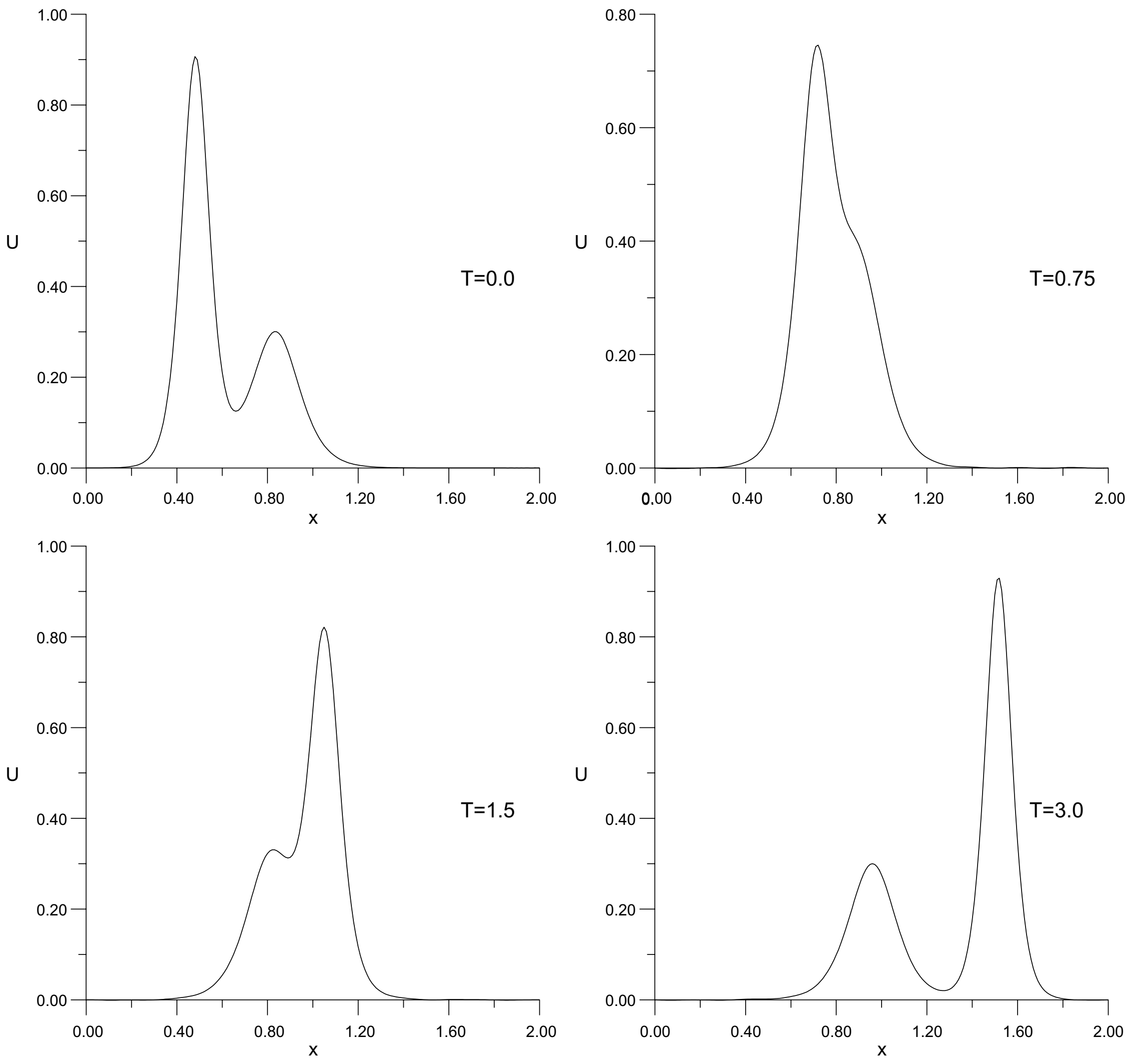

Fig. 3. Interaction of two solutions.

$0.75, 4, 5, 0.0001$ for the collocation method with MQ, G, IMQ, IQ and TPS radial basis functions, respectively.

3.3. Test problem 3

For the last text problem, initial condition

$$u(x,0) = \frac{1}{2}\left[1 - \tanh\left(\frac{|x| - 25}{5}\right)\right] \tag{14}$$

is used with boundary conditions $U(-50,t) = 0,\ U(150,t) = 0$ for $t > 0$. The breakdown of the above function into solitons will be studied with parameters $\varepsilon = 0.2,\ \mu = 0.1$ with $\Delta t = 0.05$ and $h = 0.4$. The program is run up to time $t = 800$ to observe evolution of a train of solitons. The progress of the solutions at some times is shown in Fig. 5. We see that the amplitudes of the solitons vary approximately linear and velocity of the leading soliton is in complete agreement with the theoretical values. Peak position of the leading soliton, amplitude and observed velocity at time $t = 800$ are tabulated in Table 4. The speed and amplitudes are consisted with

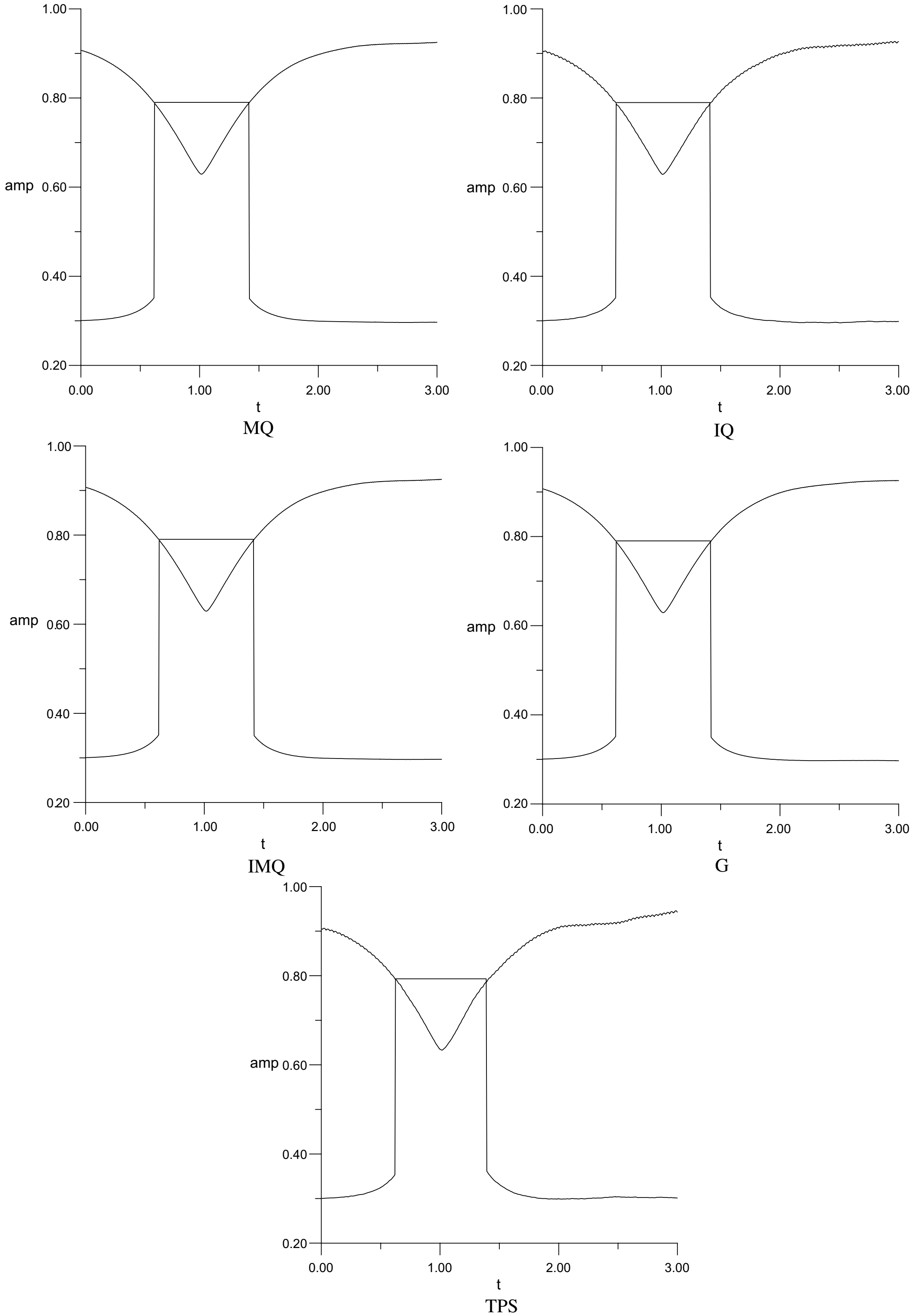

Fig. 4. Time–amplitude graphs.

Table 3
Two soliton interaction $h = 0.01$, $\Delta t = 0.005$

Method	Time	I_1	I_2	I_3	I_4
MQ	0.00	0.228080	0.107061	0.053318	0.027018
	0.75	0.228016	0.107055	0.053524	0.027358
	1.50	0.228032	0.107057	0.053453	0.027231
	3.00	0.227968	0.107061	0.053265	0.026953
G	0.00	0.228081	0.107062	0.053316	0.026950
	0.75	0.228135	0.107058	0.053312	0.027124
	1.50	0.228065	0.107059	0.053313	0.027063
	3.00	0.227734	0.107061	0.053316	0.026929
IMQ	0.00	0.228081	0.107062	0.053316	0.026952
	0.75	0.228964	0.107068	0.053307	0.027136
	1.50	0.228917	0.107072	0.053308	0.027078
	3.00	0.227399	0.107087	0.053307	0.026942
IQ	0.00	0.228081	0.107062	0.053316	0.027181
	0.75	0.228456	0.107060	0.053312	0.027131
	1.50	0.228386	0.107063	0.053314	0.027071
	3.00	0.227576	0.107069	0.053317	0.026934
TPS	0.00	0.228079	0.107062	0.053317	0.027033
	0.75	0.227689	0.107056	0.053468	0.027633
	1.50	0.227633	0.107059	0.053410	0.027407
	3.00	0.228071	0.107058	0.053274	0.027110

findings in Table 4. Invariants are given in Table 5. This solution is not produced well when the thin plate spline function is used in the collocation method. So no results of the radial basis collocation method with thin-plate spline are given in this section. Lowest errors have achieved with use of the shape parameters $c = 0.02, 100, 0.01, 0.01, 0.001$ for the radial basis functions named MQ, G, IMQ and IQ radial basis functions, respectively.

Amplitude and peak position of the leading soliton, and its speed have been tabulated in Table 4. Approximate velocity using the peak position of the leading soliton at times $t = 600$ and 800 are also documented in the same table by using the average velocity formula = ((peak pos.($t = 600$) − peak pos.($t = 800$)))/(time1($t = 600$) − time2($t = 800$)). Invariants I_1, I_2, I_3, I_4 change by less than 0.04%, 0.0008%, 0.006%, 0.05% for the algorithm with Gaussian radial basis function, 0.006%, 0.0004%, 0.0009%, 0.05% for use of multiquadratic radial basis function, 0.008%, 0.008%, 0.01%, 1.19% for inverse quadric radial basis function and 0.0006%, 0.001%, 0.002%, 0.16% for the inverse multiquadric radial basis function, respectively, when the program is run up to time $t = 800$.

3.4. Conclusion

Collocation method with radial basis functions has set up to have the numerical solution of the KDVE. Comparison of the standard radial basis functions in the collocation method shows that multiquadric radial basis function is much preferable in terms of the accuracy in getting solution of the KDVE and least accuracy is found with the collocation method with thin plate spline function. Single soliton solution and interaction of two solitons are presented well with use of the all radial basis functions. For case of evolution of solitons from the tanh type initial condition, thin plate spline collocation method is not produced solitons over the long period of run up to time $t = 800$. We have also observe that the collocation method based on both MQ and G radial basis functions produces the same accuracy with the cubic B-spline Galerkin method for getting the numerical solution of the KDVE. Disadvantage in using the RBF method is that computational cost of the proposed method is higher than the cubic B-spline Petrov Galerkin Method. Using the radial basis functions, the magnitude, profile and position of the solitons are produced well. Thus proposed method is also suitable for computation of the solutions of the KDVE.

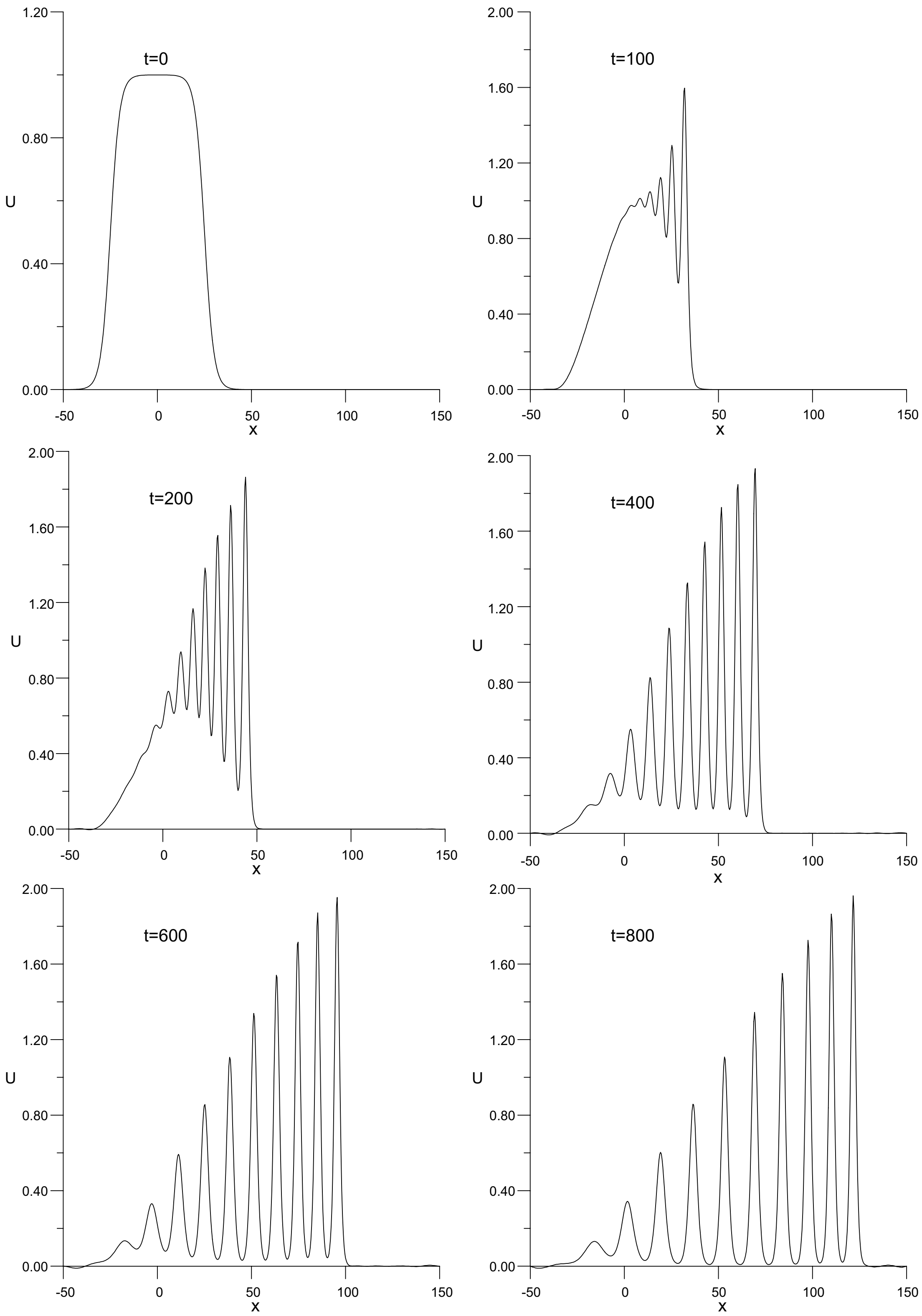

Fig. 5. The breakup of an arbitrary initial pulse into a train of solutions.

Table 4
Position, amplitude and speed of the leading soliton

Method	Position	Amplitude	$V_a = \frac{a\varepsilon}{3}$	Average velocity
MQ	121.60	1.96110	0.13074	0.13
G	121.60	1.96208	0.13080	0.13
IMQ	121.60	1.95721	0.13048	0.13
IQ	121.60	1.96203	0.13080	0.13

Table 5
Invariants for generation of solitons

Method	Time	I_1	I_2	I_3	I_4
MQ	0	50.000254	45.000503	42.300745	40.441790
	800	49.956028	45.003314	42.293530	40.080289
G	0	50.000097	45.000451	42.300677	40.441704
	800	49.963349	45.007211	42.317400	40.095789
IQ	0	50.000088	45.0004496	42.300674	40.441699
	800	49.932479	44.934811	42.188016	39.909104
IMQ	0	49.999900	45.000443	42.300661	41.015678
	800	49.995146	45.011987	42.316392	42.318768

References

[1] D.J. Korteweg-de Vries, G. de Vries, On the change in form of long waves advancing in rectangular canal and on a new type of long stationary waves, Philos. Mag. 39 (1895) 422–443.
[2] R.K. Dodd, J.C. Eilbeck, J.D. Gibbon, H.C. Morris, Solitons and Nonlinear Wave Equations, Acedemic Press, Newyork, 1982.
[3] H. Washimi, T. Taniuti, Propogation of ion acoustic solitary waves of small amplitude, Phys. Rev. Lett. 17 (1966) 996–998.
[4] L. van Wijngaarden, On the equation of motion for mixtures of liquid and gas bubbles, J. Fluid Mech. 33 (1968) 465–474.
[5] C.S. Gardner, G.K. Marikawa, The effect of temperature of the width of a small amplitude solitary wave in a collision free plasma, Comm. Pure Appl. Math. 18 (1965) 35–49.
[6] E.J. Kansa, Multiquadrics scattered data approximation scheme with applications to computational fluid-dynamics. I. surface approximations and partial derivative estimates, Comput. Math. Appl. 19 (1990) 127–145.
[7] X. Zhang, K.Z. Song, M.W. Lu, X. Liu, Meshless methods based on collocation with radial basis functions, Comput. Mech. 26 (2000) 333–343.
[8] C. Franke, R. Schaback, Solving partial differential equations by collocation using radial basis functions, Appl. Math. Comput. 93 (1998) 73–82.
[9] H. Power, V. Barraco, A comparison analysis between unsymmetric and symmetric radial basis function collocation methods for the numerical solution of the partial differential equations, Comput. Math. Appl. 43 (2002) 551–583.
[10] J. Li, Y.C. Hon, C.S. Chen, Numerical comparisons of two meshless methods using radial basis functions, Eng. Anal. Bound. Elem. 26 (2002) 205–225.
[11] J. Li, Y. Chen, D. Pepper, Radial basis function method for 1-D and 2-D groundwater contaminant transport modelling, Comput. Mech. 32 (2003) 10–15.
[12] S.A. Sarra, Adaptive radial basis function methods for time dependent partial differential equations, Appl. Numer. Math. 54 (2005) 79–94.
[13] Z. Wu, Solving PDE with radial basis function and the error estimation, in: Z. Chen, Y. Li, C.A. Micchelli, Y. Xu, M. Dekkon (Eds.), Adv. in Comput. Math, Lecture Notes on Pure and Applied Math., vol. 202, 1998.
[14] H. Wendland, Meshless Galerkin methods using radial basis functions, Math. Comput. (228) (1999) 1521–1531.
[15] Z. Wu, Y.C. Hon, Convergence error estimates in solving free boundary diffusion problem by radial basis functions method, Eng. Anal. Bound. Elem. 27 (2003) 73–79.
[16] R.A. Lorentz, F.J. Narcowich, J.D. Ward, Collocation discretizations of the transport equation with radial basis functions, Appl. Math. Comput. 145 (2003) 97–116.
[17] C. Franke, R. Schaback, Convergence order estimates of meshless collocation methods using radial basis functions, Adv. Comput. Math. 8 (1998) 381–399.
[18] S.G. Rubin, R.A. Graves, Cubic spline approximation for problems in fluid mechanics, Nasa TR R-436,Washington, DC, 1975.
[19] R.M. Miura, C.S. Gardner, M.D. Kruskal, Korteweg-de Vries equation and generalizations. II. Existence of conservation laws and constants of motion, J. Math. Phys. 6 (1968) 1204–1209.

[20] G.A. Gardner, A.H.A. Ali, L.R.T. Gardner, Simulation of solitons using quadratic spline shape functions, UCNW preprint 89.03, 1989.
[21] N.J. Zabusky, A synergetic approach to problem of nonlinear dispersive wave propagation and interaction, in: W. Ames (Ed.), Proceedings of the Symposium on Nonlinear Partial Differential Equations, Academic Press, 1967, pp. 223–258.
[22] M.E. Alexander, J.LL. Morris, Galerkin methods for some model equations for nonlinear dispersive waves, J. Comput. Phys. 30 (1979) 428–451.
[23] J.M. Sanz Serna, I. Christle, Petrov Galerkin methods for nonlinear dispersive waves, J. Comput. Phys. 39 (1981) 94–102.